ORNL/SPR-2019/1070

Dose Rate Analysis of the WCS Consolidated Interim Storage Facility

Georgeta Radulescu
Thomas M. Miller
Kaushik Banerjee
Douglas E. Peplow

August 2021

OAK RIDGE NATIONAL LABORATORY
MANAGED BY UT-BATTELLE FOR THE US DEPARTMENT OF ENERGY

ORNL/SPR-2019/1070

Nuclear Energy and Fuel Cycle Division

DOSE RATE ANALYSIS OF THE WCS CONSOLIDATED INTERIM STORAGE FACILITY

Georgeta Radulescu
Thomas M. Miller
Kaushik Banerjee
Douglas E. Peplow

Date Published: August 2021

Prepared by
OAK RIDGE NATIONAL LABORATORY
Oak Ridge, TN 37831-6283
managed by
UT-BATTELLE, LLC
for the
US DEPARTMENT OF ENERGY
under contract DE-AC05-00OR22725

CONTENTS

LIST OF FIGURES

LIST OF TABLES

ACRONYMS

ANSI/ANS	American National Standards Institute/American Nuclear Society
BWR	boiling water reactor
CFR	Code of Federal Regulations
CISF	consolidated interim storage facility
DSC	dry shielded canister
FSAR	final safety analysis report
FW-CADIS	forward-weighted consistent adjoint driven importance sampling
GTCC	greater than class C (waste)
HSM	horizontal storage module
ISFSI	independent spent fuel storage installation
LACBWR	La Crosse Boiling Water Reactor
Monte Carlo	MC
MPC	multipurpose canister
MT	metric tons
MTHM	metric tons heavy metal
NAC	Nuclear Assurance Corporation
NRC	US Nuclear Regulatory Commission
ORNL	Oak Ridge National Laboratory
PWR	pressurized water reactor
SAR	safety analysis report
SMUD	Sacramento Municipal Utility District
SNF	spent nuclear fuel
SONGS1	San Onofre Nuclear Generating Station Unit 1
SS	stainless steel
UMS	Universal Multi-Purpose (Cask) Storage
UNF-ST&DARDS	Used Nuclear Fuel—Storage, Transportation & Disposal Analysis Resource and Data Systems
VCC	vertical concrete cask
W	Westinghouse
WCS	Waste Control Specialists

ABSTRACT

This report describes a confirmatory calculation for a proposed consolidated interim storage facility (CISF) to support the US Nuclear Regulatory Commission's review of the license application submitted by the Interim Storage Partners. The scope of this report is limited to an assessment of the annual dose from direct radiation associated with Phase 1 of the Waste Control Specialists (WCS) CISF and the determination of the minimum controlled area boundary based on the 10 CFR 72.104 limit of 25 mrem annual dose to the whole body. The confirmatory dose rate calculations used the source term and shielding calculation capabilities of the SCALE 6.2.3 computer code system. The calculation method employed in the confirmatory calculations uses a detailed Monte Carlo radiation transport simulation from source to dose rate. This method differs from the two-step method used in the safety analysis report (SAR), which requires determination of the photon and neutron energy and angular distributions on the cask external surface and then the use of this surface source in a new radiation transport calculation to determine dose rate as a function of distance from the storage facility. A simulation was made using the complete site geometry (all casks present) but with only one cask containing source, and a total of 467 independent calculations were performed to obtain the dose rate maps produced by each storage cask. Basic input data and assumptions used in the SAR (e.g., cask design parameters and design basis assembly characteristics) were used in this confirmatory calculation for consistency with the SAR. Local atmospheric conditions for skyshine calculations were simulated using US standard atmosphere data, which describe average air temperature, pressure, and density as a function of altitude. The determined minimum required distances from the WCS Phase 1 CISF to a contour defined by the 25 mrem annual dose limit were approximately 623 m (0.387 miles) in the N-NE direction, 594 m (0.369 miles) in the S-SW direction, and 533 m (0.331 miles) in the E-SE direction and the W-NW direction. The annual dose results of the confirmatory calculation are in relatively good agreement with the annual dose values presented in the WCS SAR. The annual dose produced by the Phase 1 CISF at the nearest site boundary, 0.75 miles away from the CISF, was estimated by this study to be approximately 6.02E-02 ± 2.0E-04 mrem, which is significantly smaller than the 25 mrem annual dose limit provided in 10 CFR 72.104. The SAR annual dose rate value for the nearest site boundary was 7.52E-2 mrem, which included 7.73E-03 mrem due to postulated leakage of the FO-, FC-, and FF-canisters. A comparison with the dose rate values reported in the SAR for 16 detector locations, D1 through D16, on the protected area boundary is also included in this report. This comparison shows that the SAR determined higher annual dose values for detectors D1 through D14 by 12% to 45% and lower annual dose values for detectors D15 and D16 by 18% and 8%, respectively, as compared with this ORNL confirmatory calculation.

Sensitivity studies have been performed to support a comprehensive review of the application. In these studies, the effects on dose rate of the modeled air volume, density, and humidity were analyzed. The sensitivity calculations showed that the air volume used in the Monte Carlo simulations was adequate and that a larger air volume would not further increase the dose rate due to skyshine contributions. The sensitivity analysis showed that simulation of local atmospheric conditions is important for the accuracy of dose rate estimates at large distances from the facility. Air humidity was demonstrated to have negligible effects on dose rate values for the simulated local atmospheric conditions.

1. INTRODUCTION

This report describes a confirmatory dose rate calculation for a proposed consolidated interim storage facility (CISF) for spent nuclear fuel (SNF) to support the US Nuclear Regulatory Commission (NRC)'s review of the license application submitted by the Interim Storage Partners.[1,2] The scope of this report is limited to an assessment of the annual dose in air for Phase 1 of the Waste Control Specialists (WCS) CISF and the determination of the minimum controlled area boundary based on the Code of Federal Regulations (CFR) Title 10, Section 72.104,[3] limit of 25 mrem annual dose to the whole body. The WCS CISF would be located in Andrews, Texas.

The WCS Phase 1 CISF would store 5,000 metric tons of heavy metal (MTHM) SNF and up to 231.3 MT of greater-than-class C (GTCC) waste in Nuclear Assurance Corporation (NAC) vertical concrete casks (VCCs) and NUHOMS® horizontal storage modules (HSMs). Six different storage overpack systems would be used to store SNF assemblies and GTCC waste, including the NAC-Universal Multi-Purpose Storage (UMS) System,[4,5] NAC-Multi-Purpose Canister (MPC) Storage System,[6,7] MAGNASTOR Storage System,[8,9] NUHOMS®-MP187 Storage System,[10,11] Advanced Standardized NUHOMS® Storage System,[12,13] and the Standardized NUHOMS® 61BT/61BTH Type 1 Storage System.[14] The Phase 1 storage pad contains 319 VCCs and 148 HSMs and is organized in 15 arrays of VCCs and 5 arrays of HSMs. The extent of the concrete pad is 800×350 ft^2 (approximately 244×107 m^2).

The VCCs would be used to store SNF and GTCC waste currently in dry storage at the Maine Yankee (64 canisters), Connecticut Yankee (43 canisters), Yankee Rowe (16 canisters), Zion (65 canisters), and La Crosse Boiling Water Reactor (LACBWR) (5 canisters) independent spent fuel storage installations (ISFSIs), as well as future pressurized water reactor (PWR) SNF (126 canisters). The NUHOMS HSMs would be used to store SNF currently in dry storage at the San Onofre Nuclear Generating Station Unit 1 (SONGS1) (20 canisters), Sacramento Municipal Utility District (SMUD) (24 canisters), Millstone Unit 1 (48 canisters) ISFSIs, and future boiling water reactor (BWR) SNF (56 canisters).

The dose rate at a location external to a storage cask is produced by photon and neutron radiation escaping from the cask and reaching that location unobstructed or through multiple scattering interactions with nuclei/atoms in the environment (e.g., air, soil, concrete). Ample volumes of air and soil extending beyond the location of interest for dose rate calculation are typically included in the calculation model to properly simulate important radiation scattering events that contribute to the dose rate at that location. A two-step method has been used in the safety analysis report (SAR).[2] The purpose of the first step of the method was to determine energy and angular distributions on the cask external surface of the neutrons and photons exiting a storage cask. The surface source was then used in a new radiation transport calculation to determine dose rate as a function of distance up to approximately 4 miles from the WCS Phase 1 CISF. The calculation method employed in the confirmatory calculations uses a detailed Monte Carlo radiation transport simulation from source to dose rate. However, the same basic input data and assumptions used in the SAR (e.g., cask design parameters, design basis assembly characteristics, and air composition) were used in this confirmatory calculation for consistency with the SAR.

This report is organized as follows. Section 2 describes the computer codes used to calculate SNF radiation source terms and dose rate. The geometry model of the WCS Phase 1 CISF is described in Section 3. Results of sensitivity calculations determining the effects on dose rate of the input values used for air density, relative humidity, and volume are presented in Section 4. The annual dose map and the 25-mrem/yr contour determined for the WCS Phase 1 CISF are described in Section 5. A comparison to dose rate values provided in the SAR (Ref. 2, Table 9-5) is provided in Section 6. Conclusions are provided in Section 7.

2. COMPUTER CODES AND CALCULATION METHODS

The source term and shielding calculation capabilities of the SCALE 6.2.3[15] computer code system were used in the confirmatory dose rate calculations. Details of the source term and dose rate calculation methods are provided in Sections 2.1 and 2.2.

2.1 SOURCE TERM CALCULATIONS

Radiation source terms were independently generated for each design basis fuel assembly and nonfuel hardware associated with a storage system. The characteristics of the design basis fuel assembly (i.e., fuel assembly type, initial enrichment, assembly average burnup, and decay time) and nonfuel hardware were obtained from the SARs and final safety analysis reports (FSARs) prepared by cask vendors for the cask systems that will be used at the WCS CISF.

ORIGAMI,[16] a SCALE code that performs fast ORIGEN depletion calculations using pre-generated ORIGEN cross-section libraries, was used to calculate the photon and neutron sources in the fuel region and the ^{60}Co activation source in fuel assembly hardware regions and nonfuel hardware. These ORIGEN cross-section libraries, developed for the Used Nuclear Fuel—Storage, Transportation & Disposal Analysis Resource and Data Systems (UNF-ST&DARDS),[17,18] produce slightly conservative radiation source terms. The operating conditions used to generate the libraries (e.g., moderator density within the lower range of the typical moderator density values during normal operation and full fuel exposure to burnable absorber rods/control blades) were specifically selected to produce conservative nuclide concentrations for criticality calculations.[19] These operating conditions have also been demonstrated to increase the concentrations of nuclides with important contributions to neutron (e.g., ^{244}Cm) and gamma (e.g., ^{154}Eu) dose rates.[20,21,22] The concentrations of the fission product nuclide ^{137}Cs ($T_{1/2}$ = 30.07 years) and its daughter nuclide ^{137m}Ba ($T_{1/2}$ = 2.552 min), which dominates the gamma radiation source beyond 10 years of post-irradiation cooling time, were found to be insensitive to fuel operating conditions.[20]

Radiation source terms for the PWR and BWR active fuel regions were determined using the axial burnup profiles presented in Table 1. These axial profiles, also used in UNF-ST&DARDS for PWR and BWR fuel assemblies with an assembly average burnup greater than 30 and 36 GWd/MTU, respectively, are representative of axial burnup profiles for high-burnup fuel. Dose rate in air has contributions from both direct and scattered (i.e., skyshine) radiation. The contribution to the total dose rate of the scattered radiation has been shown to increase with increasing distance from a storage cask.[23] The axial burnup profile of an SNF assembly could affect the relative contributions to the total dose rate of the direct and skyshine dose rate components, but it is expected to have relatively little effect at great distance from the CISF. The axial burnup profile varies primarily as a function of fuel assembly average burnup and operating conditions, with high burnup assemblies tending to have flatter axial burnup profiles than low burnup assemblies. Relative to a pointed axial burnup profile characteristic to very low burnup assemblies, a flatter axial burnup profile would produce slightly more radiation sources near the top end of a cask that will slightly increase the skyshine radiation component and slightly decrease the direct radiation component. Conversely, a pointed axial burnup profile is expected to slightly decrease the skyshine radiation component and slightly increase the direct radiation component, relatively to a flatter axial burnup profile.

Table 1. PWR and BWR SNF assembly axial burnup profiles

PWR		BWR	
Height fraction[a]	**Axial burnup distribution**	**Height fraction[a]**	**Axial burnup distribution**
0.00 − 0.06	0.65200	0.00 – 0.04	0.23701
0.06 − 0.11	0.96700	0.04 – 0.16	1.07438
0.11 − 0.17	1.07400	0.16 – 0.24	1.29505
0.17 − 0.22	1.10300	0.24 – 0.36	1.29105
0.22 − 0.28	1.10800	0.36 – 0.48	1.24438
0.28 − 0.33	1.10600	0.48 – 0.60	1.15938
0.33 − 0.39	1.10200	0.60 – 0.72	1.08771
0.39 − 0.44	1.09700	0.72 – 0.84	0.95737
0.44 − 0.50	1.09400	0.84 – 0.92	0.66253
0.50 − 0.56	1.09400	0.92 – 1.00	0.20251
0.56 − 0.61	1.09500		
0.61 − 0.67	1.09600		
0.67 − 0.72	1.09500		
0.72 − 0.78	1.08600		
0.78 − 0.83	1.05900		
0.83 − 0.89	0.97100		
0.89 − 0.94	0.73800		
0.94 − 1.00	0.46200		

[a]From the bottom of the active fuel.

2.2 DOSE RATE CALCULATIONS

Dose rate calculations were performed with the MAVRIC shielding analysis sequence in SCALE, which employs the state-of-the-art hybrid variance reduction capabilities[24,25] developed at Oak Ridge National Laboratory (ORNL) to generate high-fidelity dose rate results. A variance reduction method referred to as *forward-weighted consistent adjoint driven importance sampling* (FW-CADIS) was used in the confirmatory calculations to estimate dose rate in the surrounding air with good statistical precision. This method (respWeighting) performs both forward and adjoint discrete ordinates calculations with the Denovo discrete ordinates code[26] to determine energy- and space-dependent source biasing and particle importance parameters. For the FW-CADIS method in MAVRIC, the user supplies a mesh for the coarse-mesh forward and adjoint deterministic calculations that are used to create the importance map and consistent biased source distribution. A mesh that captured all the details of the vast number of sources present in a CISF model would require more memory than is commonly available on current commodity computing clusters. The strategy employed in this work was to parallelize on source because the contribution to the site boundary dose rate from one source is independent of the other sources (superposition principle). A total of 467 independent calculations were performed to obtain the dose rate maps produced by each storage cask. Each simulation was made using the complete site geometry (all casks present) but with only one cask containing source. All cases were run on the Panacea cluster at ORNL. A single processor was used for each case.

The adjoint source was specified within a volume of air outside the storage pad and extending from the soil top to 2 m above the soil. This is the geometry region of the model where the dose rate is expected to be calculated with significant accuracy because variance reduction parameters were optimized for dose

rate in this region. For skyshine calculations, the volume of air in the model must be extended well beyond detector locations to include the backscattered radiation in the total dose at those locations. The volume of dry air beyond the expected location of the controlled area boundary was gradually increased until minimal effects were noticed on the total dose rate at that location. The size of the geometry model was approximately $4.2 \times 4.1 \times 2.0$ km^3. Sensitivity calculations were performed for a VCC containing Connecticut Yankee SNF using a much larger volume of air. The sensitivity calculation, presented in Section 4, shows no statistically significant difference between the results obtained with the two different air volumes. Sensitivity of dose rate to other important modeling parameters, including Denovo mesh definition, parameters describing the angular scattering in Denovo S_N calculations, tally mesh size, and computer time, was also evaluated. The values for these parameters were selected to minimize computer time requirements per particle without compromising the quality of the calculated dose rate tally.

Dose rates were calculated within a geometry mesh with a voxel size of $15.24 \times 15.24 \times 2$ m^3. The mesh tally only had one cell in the vertical direction, which extended from the top of the soil to 2 m above the soil to include the groundshine contribution above the ground. Therefore, the average dose rate within each mesh voxel was calculated and included in the dose rate map.

The American National Standards Institute/American Nuclear Society (ANSI/ANS) 6.1.1-1977 neutron and photon flux-to-dose-rate conversion factors[27] were applied to the particle flux estimated by the Monte Carlo method to obtain the dose rate.

3. FACILITY MODEL

The geometry model for the WCS Phase 1 CISF, the extent of which was approximately $4.2 \times 4.1 \times 2.0$ km^3, includes the Phase 1 storage pad, soil, and surrounding air. The analyzed storage pad configuration consisted of 467 (319 vertical and 148 horizontal) storage casks that can store up to 5,000 MTHM. This is the configuration used in the WCS shielding calculations (Ref. 28, p. 405). The design drawings and design basis fuel characteristics available for the storage systems were used to develop a SCALE model for the WCS Phase 1 CISF for consistency with the SAR model.

The inventory of GTCC waste is as follows: 4 GTCC canisters from the Zion ISFSI, 1 GTCC canister from the Yankee Rowe ISFSI, 3 GTCC canisters from the Connecticut Yankee ISFSI, 4 GTCC canisters from the Maine Yankee ISFSI, and 1 Rancho Seco GTCC canister. In this analysis, all GTCC waste was modeled as SNF for simplicity and conservatism.[2]

The models developed for the three unique NAC VCC designs (NAC-UMS®, NAC-MPC, and MAGNASTOR CC4) and three unique NUHOMS® HSM designs (Models 102, Advanced, and 80) are described in Sections 3.1 through 3.6. The figures in these sections show the degree of geometry detail represented in the cask models. The design basis fuel assembly was typically modeled as four axial regions: the upper end fitting region, upper gas plenum region, active fuel region, and lower end fitting region. Each axial region was represented as homogenous material within its geometry boundary with a mass density and elemental compositions derived from assembly materials and weights. The complete WCS Phase 1 CISF model is presented in Section 3.7.

3.1 NAC-UMS® SYSTEM

The NAC-UMS® system would be used to store the 64 Maine Yankee SNF and GTCC waste canisters currently stored at the Maine Yankee ISFSI. Other future PWR SNF that will be located in the WCS Phase 1 CISF would also be stored in NAC-UMS® VCCs.[28] The design basis PWR fuel assembly for the shielding evaluation of the NAC-UMS® system is the Westinghouse (W) 17 × 17 Std with an initial

uranium mass of 467.1 kg, an assembly average burnup of 40 GWd/MTU, an initial enrichment of 3.7 wt% ^{235}U, and a 5-year cooling time (Ref. 2, Appendix F.1). The canister designated for this fuel assembly is the NAC-UMS® Class 1 transportable storage canister. A burnable poison rod assembly was assumed in each fuel assembly. The assumed cobalt impurity concentration in the fuel assembly hardware and nonfuel hardware was 1.2 g/kg (Ref. 5). Vertical and horizontal cross-sectional views of the model developed for the NAC-UMS® VCC are shown in Figure 1. The input data used to develop the model for the NAC-UMS® VCCs (Maine Yankee and Standard) were taken from (Ref. 5, Section 5).

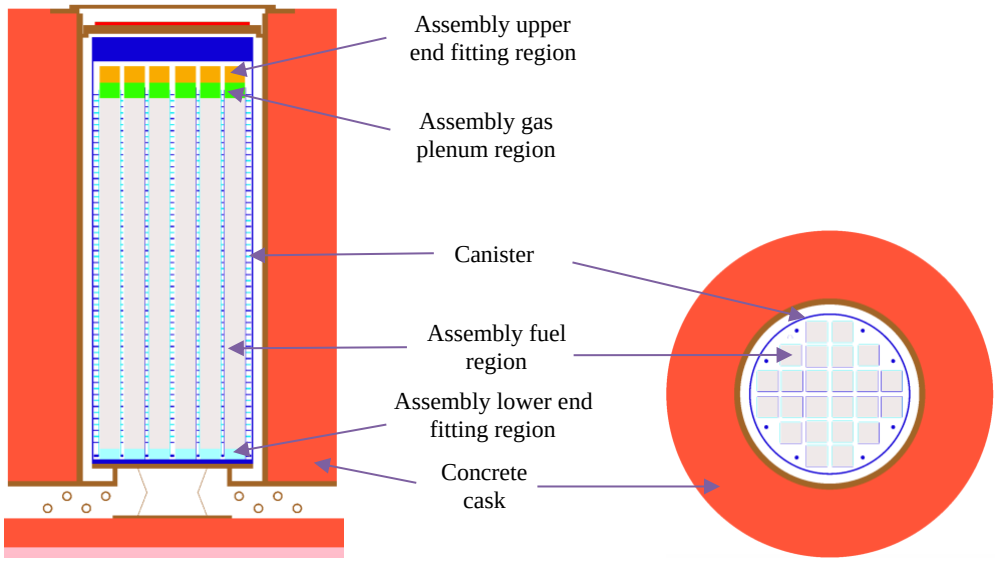

Figure 1. Vertical (a) and horizontal (b) cross-sectional views of the NAC-UMS® VCC model.

3.2 NAC-MPC SYSTEM

The NAC-MPC system would be used to store the SNF and GTCC waste currently in storage at the Connecticut Yankee (46 canisters), Yankee Rowe (16 canisters), and LACBWR (5 canisters) ISFSIs. The NAC-MPC system includes an MPC type for each of these fuel types: the Connecticut Yankee-MPC (see Section 3.2.1), Yankee-MPC (see Section 3.2.2), and MPC-LACBWR (see Section 3.2.3).

3.2.1 Connecticut Yankee-MPC

The Connecticut Yankee-MPC accommodates up to 26 fuel assemblies irradiated in the Haddam Neck Nuclear Power Plant reactor. The design basis fuel assembly for the shielding evaluation of this canister was the Zircaloy-clad XHN15WZ[29] fuel assembly type with an assembly average burnup of 43 GWd/MTU, an initial enrichment of 3.59 wt% ^{235}U, and a 5-year cooling time.[7] The initial uranium mass in the fuel assembly was 422 kg. The assumed cobalt impurity concentration in the fuel assembly hardware and nonfuel hardware was 1.2 g/kg (Ref. 7). Vertical and horizontal cross-sectional views of the model developed for the NAC-MPC VCC containing Connecticut Yankee SNF are shown in Figure 2.

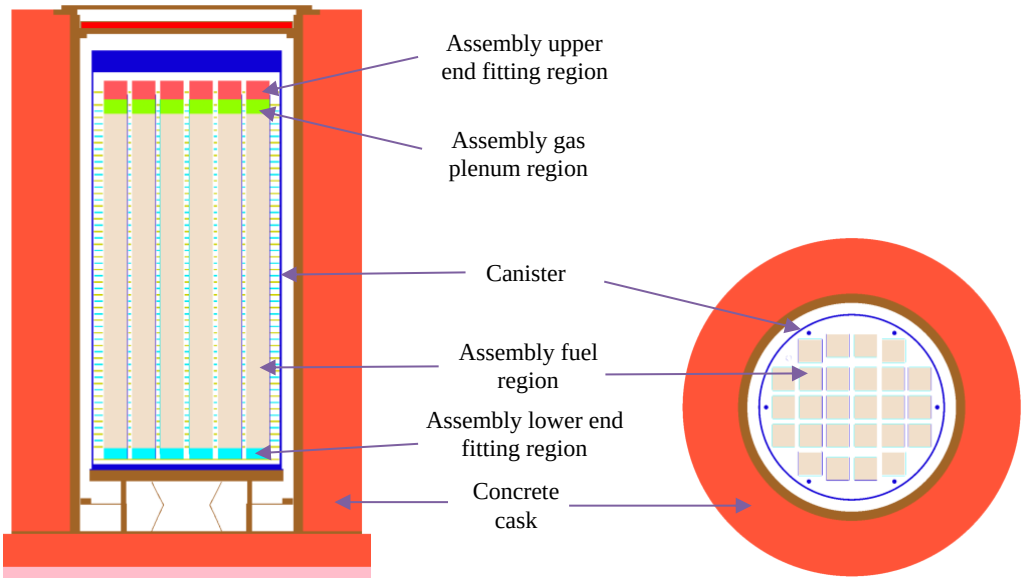

Figure 2. Vertical (a) and horizontal (b) cross-sectional view of the geometry model for the NAC-MPC VCC containing Connecticut Yankee SNF.

3.2.2 Yankee-MPC

The Yankee-MPC accommodates up to 36 fuel assemblies irradiated in the Yankee Rowe Nuclear Power Plant reactor. The design basis fuel assembly for the shielding evaluation of this canister was the XYR16C[29] fuel assembly type with an assembly average burnup of 36 GWd/MTU, an initial enrichment of 3.7 wt% ^{235}U, and an 8-year cooling time.[7] The initial uranium mass in the fuel assembly was 239.4 kg. The assumed cobalt impurity concentration in the fuel assembly hardware and nonfuel hardware was 1.2 g/kg (Ref. 7). Vertical and horizontal cross-sectional views of the model developed for the NAC-MPC VCC containing Yankee Rowe SNF are shown in Figure 3.

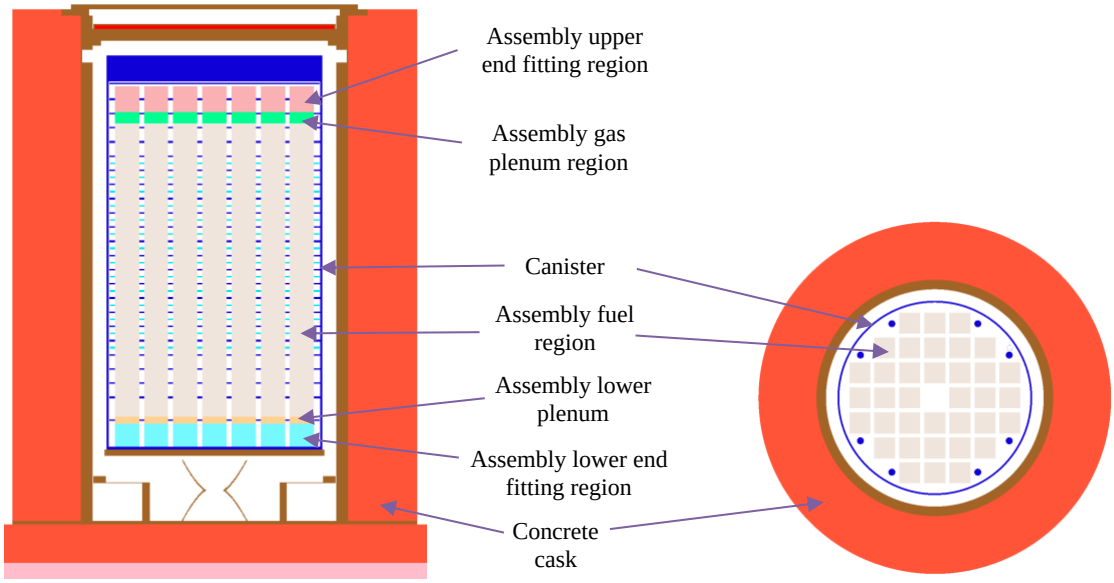

Figure 3. Vertical (a) and horizontal (b) cross-sectional view of the geometry model for the NAC-MPC VCC containing Yankee Rowe SNF.

3.2.3 MPC-LACBWR

The Yankee-MPC was modeled in place of the MPC-LACBWR (see Section 3.2.2). This is a conservative approach because the Yankee-MPC produces higher maximum external dose rates than the MPC-LACBWR, as shown in the NAC-MPC FSAR (Ref. 7, Tables 5.1.1-1, 5.A.1-1, and 5.A.1-2). This approach was adopted for simplicity and conservatism.

3.3 NAC MAGNASTOR SYSTEM

The MAGNASTOR system would be used to store Zion SNF and GTCC waste. The transportable storage canister has a 37-PWR fuel assembly capacity. The design basis PWR fuel assembly has a decay heat of 40 kW/canister.[8] The characteristics of the design basis fuel assembly used in source term calculations are the W 15 × 15 fuel type (Zion fuel assembly type), an initial uranium mass of 467.1 kg, a 2.5 wt% ^{235}U enrichment, an assembly average burnup value of 37.5 GWd/MTU, and a 4.1-year decay time. A burnable poison rod assembly was assumed in each fuel assembly. The assumed cobalt impurity concentration in the fuel assembly hardware and nonfuel hardware was 0.8 g/kg (Ref. 8). Vertical and horizontal cross-sectional views of the model developed for the MAGNASTOR VCC in a CC4 shielding configuration are shown in Figure 4.

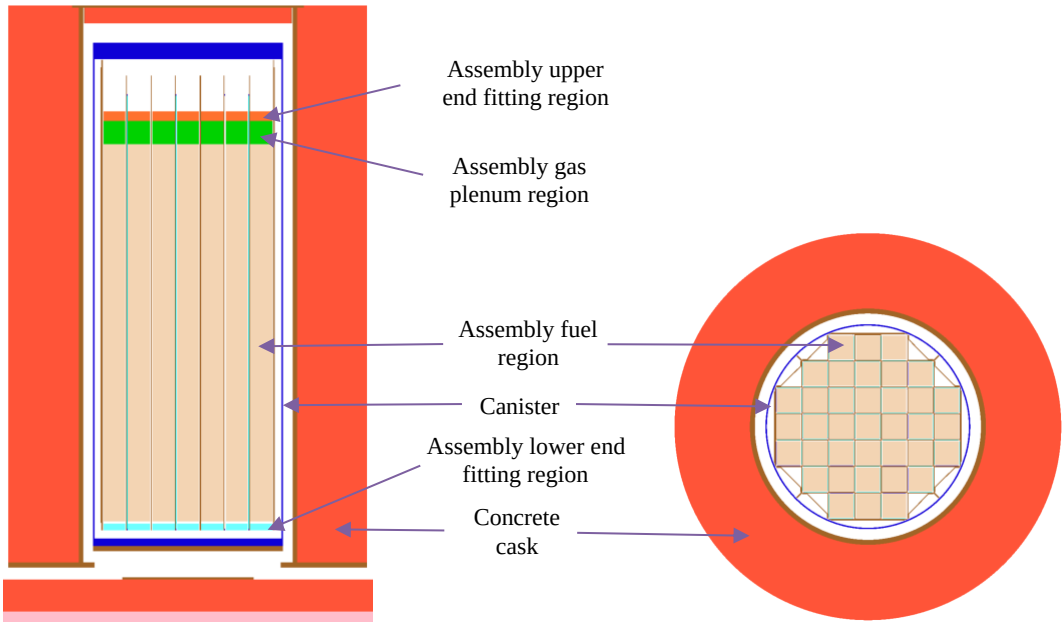

Figure 4. Vertical (a) and horizontal (b) cross-sectional views of the model for the MAGNASTOR VCC containing Zion SNF assemblies.

3.4 NUHOMS® HSM MODEL 102

The NUHOMS® HSM Model 102 would be used to store SNF from the Millstone Unit 1 power plant (48 61BTH Type 1 dry shielded canisters [DSCs]) and future BWR SNF (56 61BT DSCs). These DSCs have a capacity of 61 BWR fuel assemblies. The design basis fuel assembly type for the shielding evaluation of this canister was the General Electric (GE) 7 × 7 Type 2,3 fuel assembly.[14] The initial uranium mass in the fuel assembly was 198 kg. The assumed cobalt impurity concentration in the fuel assembly hardware was 0.8 g/kg for stainless steel (SS) and 4.7 g/kg for Inconel.[17]

The 61BT DSC requires different fuel assembly characteristics for gamma and neutron source term calculations, as determined in the safety analysis.[14] The SAR performed a source term analysis for a GE 7 × 7 assembly using four different combinations of burnup, initial enrichment, and post-irradiation cooling time to determine the set of parameters producing bounding gamma and neutron radiation sources for the analyzed cases. Based on this study, the characteristics of the design basis fuel assembly for gamma source term calculations are an assembly average burnup of 27 GWd/MTU, an initial enrichment of 2 wt% ^{235}U, and a 5-year cooling time. The characteristics of the design basis fuel assembly for neutron source term calculations are an assembly average burnup of 35 GWd/MTU, an initial enrichment of 2.65 wt% ^{235}U, and an 8-year cooling time.

The 61BTH Type 1 DSC requires a 3-heat load zoning. For the central and intermediate zones, the fuel assembly has an assembly average burnup of 62 GWd/MTU, an initial enrichment of 2.6 wt% ^{235}U, and a 21.4-year cooling time. For the outer intermediate zone, the fuel assembly has an assembly average burnup of 25 GWd/MTU, an initial enrichment of 1.0 wt% ^{235}U, and a 3.2-year cooling time. For the peripheral zone, the fuel assembly has an assembly average burnup of 25 GWd/MTU, an initial enrichment of 0.9 wt% ^{235}U, and a 3-year cooling time.

Vertical and horizontal cross-sectional views of the model developed for the NUHOMS® HSM Model 102 are shown in Figure 5.

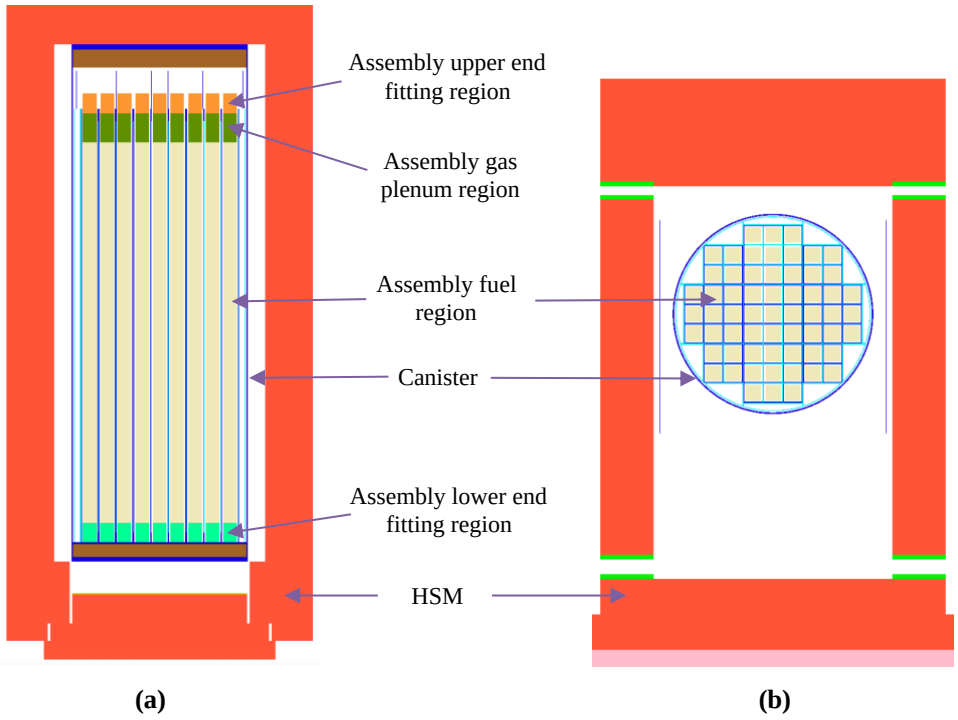

Figure 5. Horizontal (a) and vertical (b) cross-sectional views of the model for the NUHOMS® HSM Model 102 containing Millstone Unit 1 SNF assemblies.

3.5 NUHOMS® ADVANCED HSM

The NUHOMS® Advanced HSM would be used to store SNF from the SONGS1 power plant (20 24PT1 DSCs). The 24PT1 DSC has a capacity of 24 fuel assemblies. The design basis fuel assembly type for the shielding evaluation of this canister was the W 14 × 14 fuel assembly.[13] The assumed cobalt impurity concentration in fuel assembly and nonfuel hardware was 0.8 g/kg for SS and 4.7 g/kg for Inconel.[17] The characteristics of the design basis fuel assembly used in source term calculations were an initial uranium mass of 375 kg, a 3.8 wt% ^{235}U enrichment, an assembly average burnup value of 45 GWd/MTU, and a 10-year decay time.

Horizontal and vertical cross-sectional views of the model developed for the NUHOMS® Advanced HSM are shown in Figure 6.

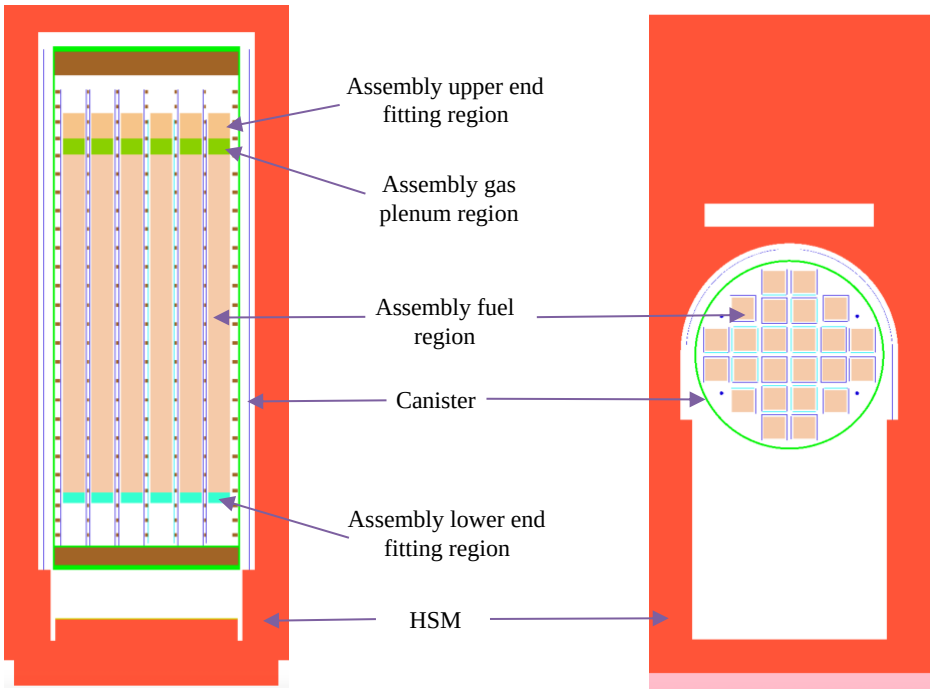

Figure 6. Horizontal (a) and vertical (b) cross-sectional views of the model for the NUHOMS® Advanced HSM containing SONGS1 SNF assemblies.

3.6 NUHOMS® HSM MODEL 80

The NUHOMS® HSM Model 80 would be used to store SNF from the Rancho Seco power plant (24 DSCs). The FC-DSC type with a 24-fuel assembly capacity was modeled. The design basis fuel assembly type for the shielding evaluation of this canister was the Babcock & Wilcox 15 × 15 fuel assembly with an initial uranium mass of 464 kg.[10,11] The DSC requires different fuel assembly characteristics for gamma and neutron source term calculations. The characteristics of the design basis fuel assembly for gamma source term calculations were an assembly average burnup of 34.143 GWd/MTU, an initial enrichment of 3.21 wt% ^{235}U, and a 7-year cooling time. The characteristics of the design basis fuel assembly for neutron source term calculations were an assembly average burnup of 38.268 GWd/MTU, an initial enrichment of 3.18 wt% ^{235}U, and a 13-year cooling time. The assumed cobalt impurity concentration in fuel assembly and nonfuel hardware was 0.8 g/kg for SS and 4.7 g/kg for Inconel.[17] Horizontal and vertical cross-sectional views of the model developed for the NUHOMS® HSM Model 80 are shown in Figure 7.

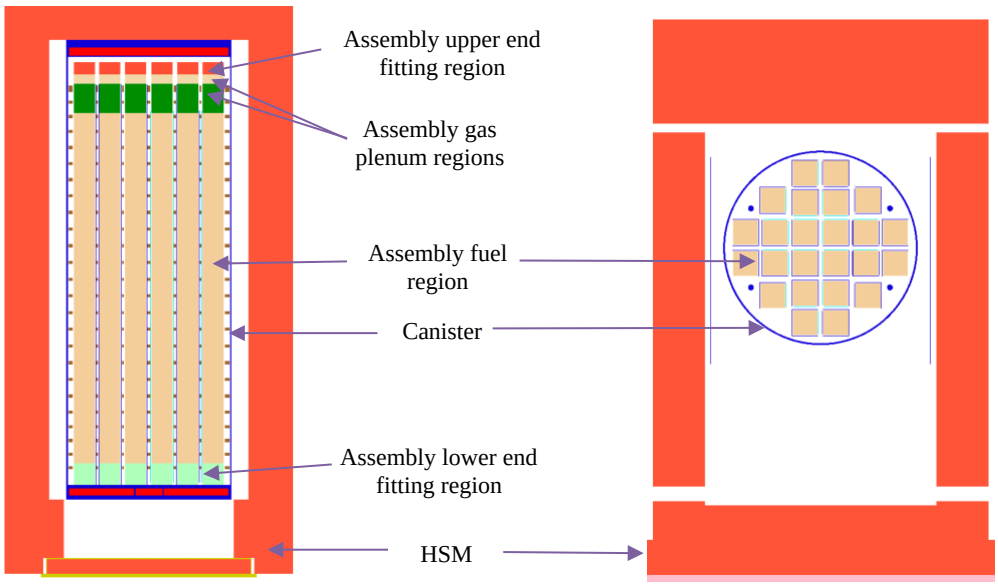

Figure 7. Horizontal (a) and vertical (b) cross-sectional views of the model for the NUHOMS® HSM Model 80 containing Rancho Seco SNF assemblies.

3.7 WCS PHASE 1 CISF MODEL

The WCS Phase 1 CISF model includes the Phase 1 storage pad, surrounding air, and soil. A three-dimensional view of the Phase 1 storage pad model is shown in Figure 8. The extent of the concrete pad was 800 × 350 ft^2 (approximately 244 × 107 m^2). The thickness of the concrete pad was 30 cm, and the soil was modeled to 1 m in depth to account for radiation scattering and absorption in soil. The extent of the air volume in the model was 6560 ft (2.0 km) in the X and Y directions beyond each side of the storage pad and 6560 ft (2.0 km) above the concrete pad.

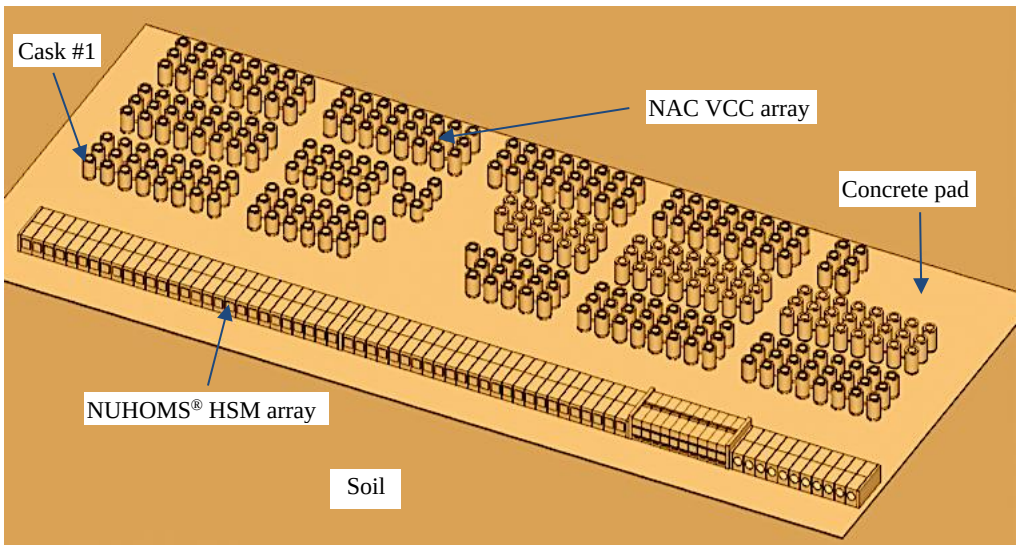

Figure 8. Three-dimensional view of the Phase 1 storage pad model.

The mass density and elemental concentrations of concrete, soil, and air used in the computational models of the current analysis are shown in Table 2. The air column in the geometry model was subdivided into 40 vertical layers, each layer 50 m high, with decreasing air density values (See Table 3) from bottom to top based on the US standard atmosphere data.[30] The concrete and carbon steel compositions were taken from the safety analysis[28] and the soil composition was taken from Ref. [31]. All isotopic concentrations were assumed to be natural isotopic concentrations as implemented in the SCALE code.[15] The sensitivity analysis in Section 4 provides details about the simulated atmospheric conditions.

Table 2. Air, soil, concrete, and carbon steel material descriptions

	Elemental weight fractions													Density (g/cm^3)
	H	**C**	**N**	**O**	**Na**	**Al**	**Mg**	**Si**	**K**	**Ca**	**Ti**	**Mn**	**Fe**	
Dry air		0.0001	0.7651	0.2348										See Table 3
Soil		0.013		0.514	0.006	0.069	0.013	0.271	0.014	0.051	0.005	0.001	0.056	1.52
Concrete	0.010			0.532	0.029	0.034		0.337		0.044			0.014	2.3227
Carbon steel		0.01											0.99	7.8212

4. SENSITIVITY CALCULATIONS

The dose rate at each location of interest is the total of the dose rate produced by the direct radiation, the dose rate produced by the radiation scattered in air (i.e., skyshine), and the dose rate produced by radiation that reemerges into the air as a result of scattering within the ground (i.e., groundshine). These dose components are affected by local environment and weather conditions. Air density varies as a function of altitude and air relative humidity could vary because of local weather conditions. Therefore, a series of sensitivity calculations were performed to determine the impact on dose rate of the air volume, density, and relative humidity used in the CISF model. The sensitivity calculation model included the complete site geometry and a single canister (Connecticut Yankee-MPC) with SNF radiation sources, which is identified as cask #1 on Figure 8. Dry air of 1.2-kg/m^3 mass density was used as the base case in these studies. Dry air with a mass density of 1.2 kg/m^3 was used in the initial version of the safety application.[28] The density of air is 1.225 kg/m^3 at sea level and 15 degrees C.

The effects of the modeled air volume on annual dose are presented in Section 4.1 based on dose rate results from calculations using two significantly different air volumes. This sensitivity calculation demonstrates that the WCS Phase 1 CISF geometry model included sufficient air volume to facilitate skyshine contributions to dose rate. The effect on dose of humid air relative to dry air and the effect of lower air density relative to the base case were analyzed in Section 4.2. The effects of local average atmospheric conditions relative to the base case are analyzed in 4.3.

The groundshine contribution to the total dose rate has been shown to be relatively small if the total dose rate is dominated by the gamma radiation[32] because the soil has small backscattering effects on photons. However, it has been shown that soil with lower amounts of hydrogen in its composition (i.e., very dry soil) increases the neutron dose rate near ground surface.[32] Therefore, the CISF model in this confirmatory analysis used a soil composition without hydrogen to increase the groundshine contribution to the neutron dose rate.

4.1 AIR VOLUME IN THE SKYSHINE CALCULATION MODEL

The size of the WCS Phase 1 CISF geometry model used in the confirmatory analysis was 4.2 × 4.1 × 2.0 km^3. In this model, the extent of the surrounding air in the ±X and ±Y directions was 2.0 km from each side of the pad and 2.0 km above the concrete storage pad in the Z direction. The WCS Phase 1 CISF geometry model used in the confirmatory analysis was compared with a geometry model with a size of approximately 2.7 × 2.6 × 0.96 km^3. In this model, the extent of the surrounding air in the ±X and ±Y directions was 1.234 km from each side of the pad and 0.96 km above the concrete storage pad in the Z direction.

The ratio of annual dose calculated with the 4.2 × 4.1 × 2.0 km^3 model to the annual dose calculated with the 2.7 × 2.6 × 0.96 km^3 model and associated two sigma statistical error is represented in Figure 9 as a function of distance from the storage pad along the X axis through the cask #1 location and in Figure 10 as a function of distance from the storage pad along the Y axis through the cask #1 location. These graphs show no statistically significant differences between the annual dose values based on the two different geometry sizes.

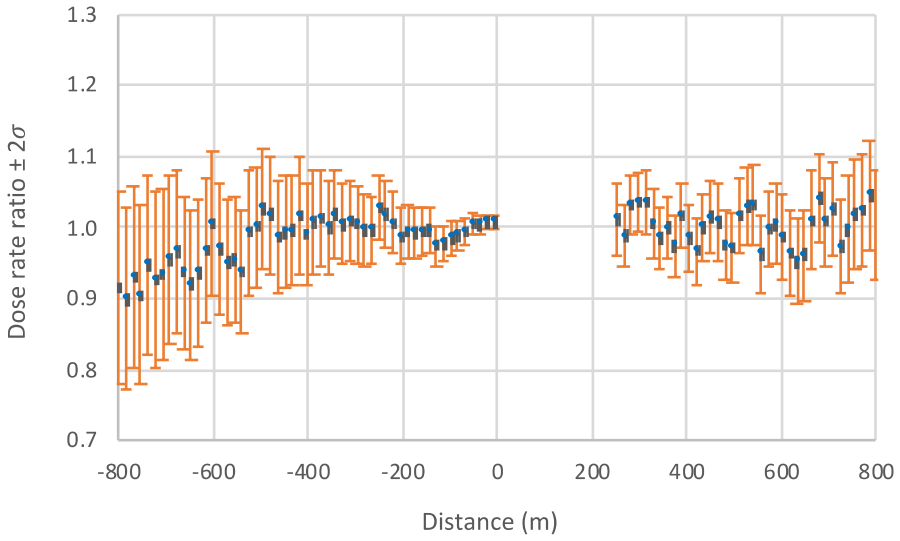

Figure 9. Ratio of annual dose from the 4.2 × 4.1 × 2.0 km^3 model to annual dose from the 2.7 × 2.6 × 0.96 km^3 model and associated two sigma statistical error as a function of distance from the storage pad along the X axis through the cask #1 location.

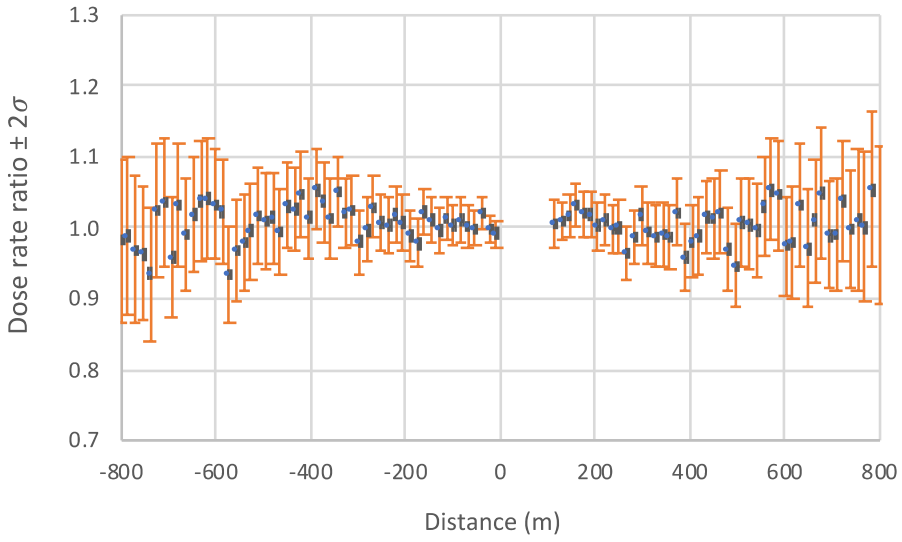

Figure 10. Ratio of annual dose from the 4.2 × 4.1 × 2.0 km^3 model to annual dose from the 2.7 × 2.6 × 0.96 km^3 model and associated two sigma statistical error as a function of distance from the storage pad along the Y axis through the cask #1 location.

4.2 DOSE SENSITIVITY TO AIR DENSITY AND HUMIDITY

Air density varies with altitude because of changes in atmospheric temperature and pressure with altitude. The amount of water vapor in air also affects air density and composition. The effects on dose rate of air density decrease with altitude is analyzed in this section.

4.2.1 Air Density Decrease

A decrease in the dry air density would have significant impact on dose rate because it reduces radiation attenuation as compared with the nominal dry air density. The effect of air density reduction on the annual dose from cask #1 is illustrated in Figure 11 using dry air of 9.6E-04 g/cm^3 (20% density reduction from the dry air density of 0.0012 g/cm^3). This density reduction is considered unrealistic for the WCS facility location, but it is used in the sensitivity calculations for information only to illustrate how significant the effects of air density changes could be on radiation dose. The air composition was not changed from that of the dry air shown in Table 2. The annual dose in air as a function of dry air density and distance from the storage pad along the X axis through the cask center is presented in Figure 11. At ~500 m and 800 m from the pad, the annual dose values would be ~70% and 180% higher if the model used a 20% lower dry air density.

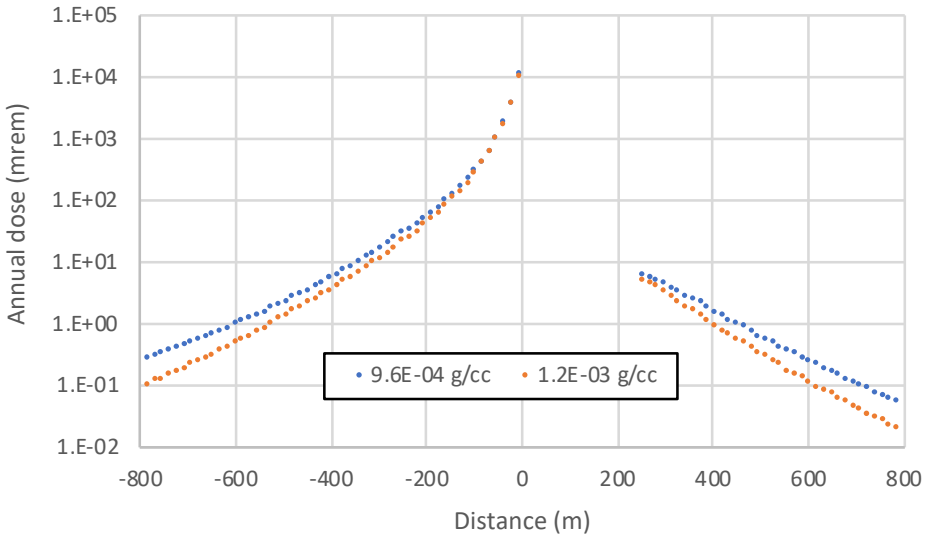

Figure 11. Effects of dry air density variation on annual dose as a function of distance from the storage pad along the Y axis through the cask #1 location.

4.2.2 Sensitivity to Air Humidity

The main components of dry air are nitrogen (~78%) and oxygen (~21%). Humid air weighs less than dry air at the same temperature because a fraction of dry air is replaced by water and the molecular weight of dry air (~28.56 g/mole) is higher than that of moist air (e.g., that would be 27.50 g/mole for moist air consisting of 90% dry air and 10% H_2O). Therefore, radiation attenuation would be slightly lower in humid air than in dry air of the same density.

A calculation was performed for cask #1 using air of 1.2-kg/m^3 density with a relative humidity of 90% and a temperature of 30°C at normal pressure. The annual dose in air as a function of distance along the Y axis through the cask is presented in Figure 12. All relative statistical errors were less than 10%, with most relative statistical errors being less than 5%. The dose values produced by the model with humid air are slightly higher than the dose values produced by the model with dry air beyond ~400 m from the storage pad. Beyond this distance, the difference between the dose values produced by the model with humid air and those produced by the model with dry air increases with increasing distance. This difference is ~10% at 500 m from the storage pad and ~20% at 800 m from the storage pad.

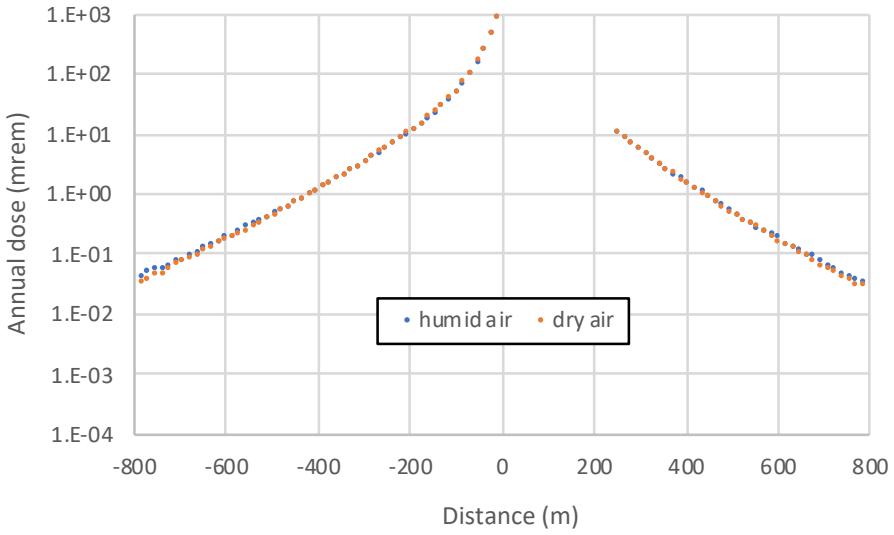

Figure 12. Effects of dry and humid air on annual dose as a function of distance from the storage pad along the Y axis through the cask #1 location.

4.3 SIMULATED LOCAL ATMOSPHERIC CONDITIONS

Dry air with a mass density of 1.2 kg/m^3 was used in the initial version of the safety application.[28] This air density value is representative for an altitude of approximately 200 m.[30] Because the altitude for the WCS CISF is 3,169 ft (~966 m), a sensitivity study was conducted to determine the effects of local atmospheric conditions on dose rate generated by cask #1. Local atmospheric conditions were simulated using US standard atmosphere data,[30] which describe average air temperature, pressure, and density as a function of altitude. The US standard air density values are presented in Table 3 as a function of altitude for the relevant altitudes of 950 m to 2,950 m. For this altitude change, standard air temperature varies from approximately 9 °C to -4 °C (48 °F to 25 °F).

Annual dose maps were generated for the pad model with 1) a uniform air density of 1.2 kg/m^3 (i.e., base case) and 2) the air column subdivided into 40 vertical layers, each layer 50 m high, with decreasing air density values from bottom to top based on the US standard atmosphere data. The dose rate values and associated 2 sigma statistical errors are presented in Table 4 for the detector locations D1 through D16 identified in Ref. 2, Figure 9-1. Table 4 also provides the ratio of dose rate produced by simulated local atmospheric conditions to dose rate from the base case. Generally, the dose rate ratio increases with increasing distance from the cask. This increase was ~ 45% at 1 km and ~ 70% at 1.7 km from the pad. The simulated local atmospheric conditions generated higher dose rate values than the base case, by a factor of 1.02 ± 0.03 at detector location D1 to 1.44 ± 0.16 at detector location D9. However, dose rate from cask #1 significantly decreased from ~1.7E-02 mrem/h at detector location D1 to ~1.8E-06 mrem/h at detector location D9.

The amount of water vapor in air also affects air density and composition, but to a lesser extent than air density, as shown in Sect. 4.2.2. For the same relative humidity, the absolute amount of water vapor in cold air is lower than the absolute amount of water vapor in warm air. Therefore, the effects of humid air relative to dry air for the local atmospheric conditions (i.e., 48 °F to 25 °F) are expected to be smaller than those shown in Sect. 4.2.2. The dose rate produced by cask #1 was calculated using the multi-layer air model with humid air of varying density. Two cases were evaluated assuming relative humidity values of 50% and 100%. The altitude-dependent humid air densities were determined with the Air Density

Calculator provided by a meteorological weather station.[33] The effects of air humidity relative to the multi-layer dry air model, shown in Figure 13, were within statistical uncertainties for the two cases.

Table 3. US standard atmosphere: air density as a function of altitude

Altitude (m)	Air density (kg/m^3)	Altitude (m)	Air density (kg/m^3)
950	1.1171		
1000	1.1117	2000	1.0065
1050	1.1062	2050	1.0015
1100	1.1008	2100	0.99642
1150	1.0954	2150	0.99141
1200	1.0900	2200	0.98642
1250	1.0846	2250	0.98145
1300	1.0793	2300	0.97649
1350	1.0739	2350	0.97156
1400	1.0686	2400	0.96664
1450	1.0633	2450	0.96175
1500	1.0581	2500	0.95687
1550	1.0528	2550	0.95201
1600	1.0476	2600	0.94717
1650	1.0424	2650	0.94235
1700	1.0372	2700	0.93755
1750	1.0320	2750	0.93277
1800	1.0269	2800	0.92800
1850	1.0218	2850	0.92326
1900	1.0167	2900	0.91853
1950	1.0116	2950	0.91382

Ref. [30].

Table 4. Effects of simulated local atmospheric conditions on dose rate relative to the base case (dry air with a mass density of 1.2 kg/m^3)

	Detector location coordinates[a]		Dose rate (mrem/h)		
Detector	X (m)	Y (m)	Local atmospheric conditions	Air density of 1.2 kg/m^3	Dose rate ratio[b]
D1	-101	122	1.69E-02 ± 3.16E-04	1.65E-02 ± 3.83E-04	1.02 ± 0.03
D2	-101	244	3.77E-03 ± 1.05E-04	3.52E-03 ± 1.29E-04	1.07 ± 0.05
D3	-101	366	6.11E-04 ± 2.27E-05	5.75E-04 ± 2.80E-05	1.06 ± 0.07
D4	-101	488	1.34E-04 ± 6.62E-06	1.09E-04 ± 6.03E-06	1.23 ± 0.11
D5	-101	619	2.84E-05 ± 1.38E-06	2.19E-05 ± 1.30E-06	1.30 ± 0.13
D6	122	619	1.65E-05 ± 7.78E-07	1.24E-05 ± 6.94E-07	1.32 ± 0.13
D7	259	619	1.19E-05 ± 5.51E-07	8.60E-06 ± 4.72E-07	1.38 ± 0.14
D8	396	619	6.08E-06 ± 2.57E-07	4.30E-06 ± 2.34E-07	1.41 ± 0.14
D9	619	619	1.77E-06 ± 8.57E-08	1.23E-06 ± 7.14E-08	1.44 ± 0.16
D10	619	488	3.72E-06 ± 1.62E-07	2.74E-06 ± 1.43E-07	1.36 ± 0.13
D11	619	366	6.96E-06 ± 2.91E-07	4.84E-06 ± 2.28E-07	1.44 ± 0.13
D12	619	244	9.93E-06 ± 4.30E-07	7.51E-06 ± 3.66E-07	1.32 ± 0.11
D13	619	122	1.26E-05 ± 5.41E-07	9.30E-06 ± 4.46E-07	1.35 ± 0.12
D14	396	-122	1.47E-04 ± 4.68E-06	1.23E-04 ± 4.16E-06	1.19 ± 0.07
D15	259	-122	6.40E-04 ± 1.60E-05	5.91E-04 ± 1.75E-05	1.08 ± 0.05
D16	122	-122	1.83E-03 ± 4.13E-05	1.73E-03 ± 4.94E-05	1.06 ± 0.04

[a]Relative to storage pad corner A identified in Figure 16, the coordinates of which are X=0 m and Y=0 m.

[b]Ratio of dose rate based on simulated local atmospheric conditions to dose rate based on uniform dry air with a mass density of 1.2 kg/m^3 (base case). The two-sigma statistical error is provided for dose rate and dose rate ratio values.

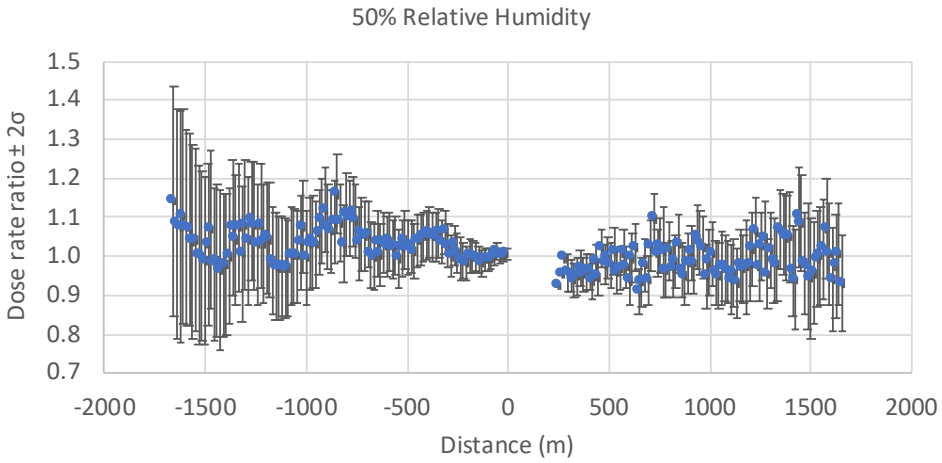

(a)

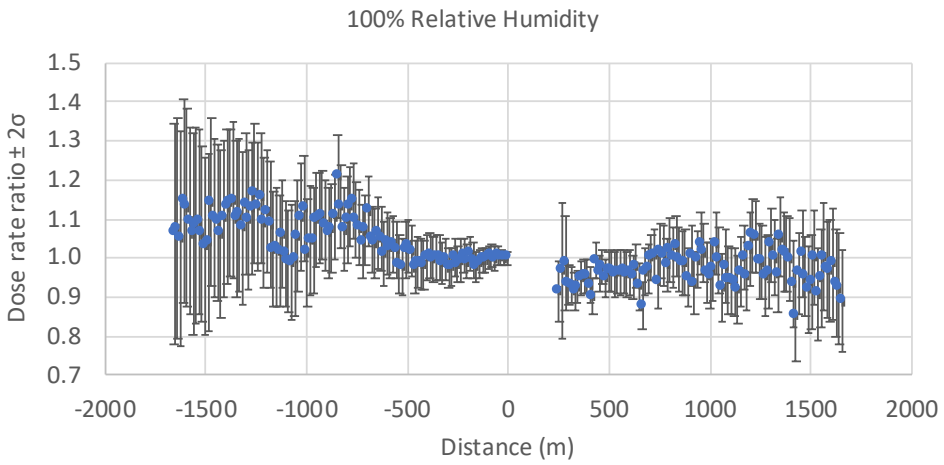

(b)

Figure 13. Effects of humid air relative to dry air for simulated weather conditions on annual dose as a function of distance from the storage pad along the X axis through the cask #1 location: a) 50% relative humidity and b) 100% relative humidity.

5. ANNUAL DOSE RESULTS

The annual dose map for the WCS Phase 1 CISF and surrounding air is presented in Figure 14. This annual dose map was obtained by summing the uncorrelated space-dependent dose rate values of the mesh tallies from the 467 separate calculations using the MAVRIC utility mtAdder.[15] The relative statistical error map associated with the dose values is shown in Figure 15. In all these calculations, the size of the model was approximately $4.2 \times 4.1 \times 2.0$ km^3 and the air density is provided in Table 3. The dose rate calculation was optimized for the spatial region outside the storage pad, which means that the dose values inside the rectangle in Figure 14 might not be reliable. As seen in Figure 15, the relative statistical errors associated with dose values are less than 5%, 10%, and 20% for most of the mesh up to 1-km, 1.7-km, and 2-km distance from the pad, respectively. At locations with an approximate annual dose of 25 mrem, this relative statistical error was approximately 1%. This statistical uncertainty was considered in determining the location of the contour defined by an annual dose of 24.7 (i.e., 25–3σ) mrem, where the 10 CFR Part 72.104 annual dose limit would be met as determined in this analysis for the 5,000-MTHM WCS Phase 1 CISF. The dose contour is shown in Figure 16, along with the distance from the pad boundary to the 25-mrem/yr contour. Based on the ORNL calculations, the minimum distance from the Phase 1 storage pad to the 25-mrem/yr contour is 623 m (0.387 miles) in the N-NE direction, 594 m (0.369 miles) in the S-SW direction, and 533 m (0.331 miles) in the E-SE direction and the W-NW direction (see Figure 16). The dose rates in mrem/yr along the X and Y axes as a function of distance from the Phase 1 storage pad boundary are shown in Figure 17 and Figure 18, respectively.

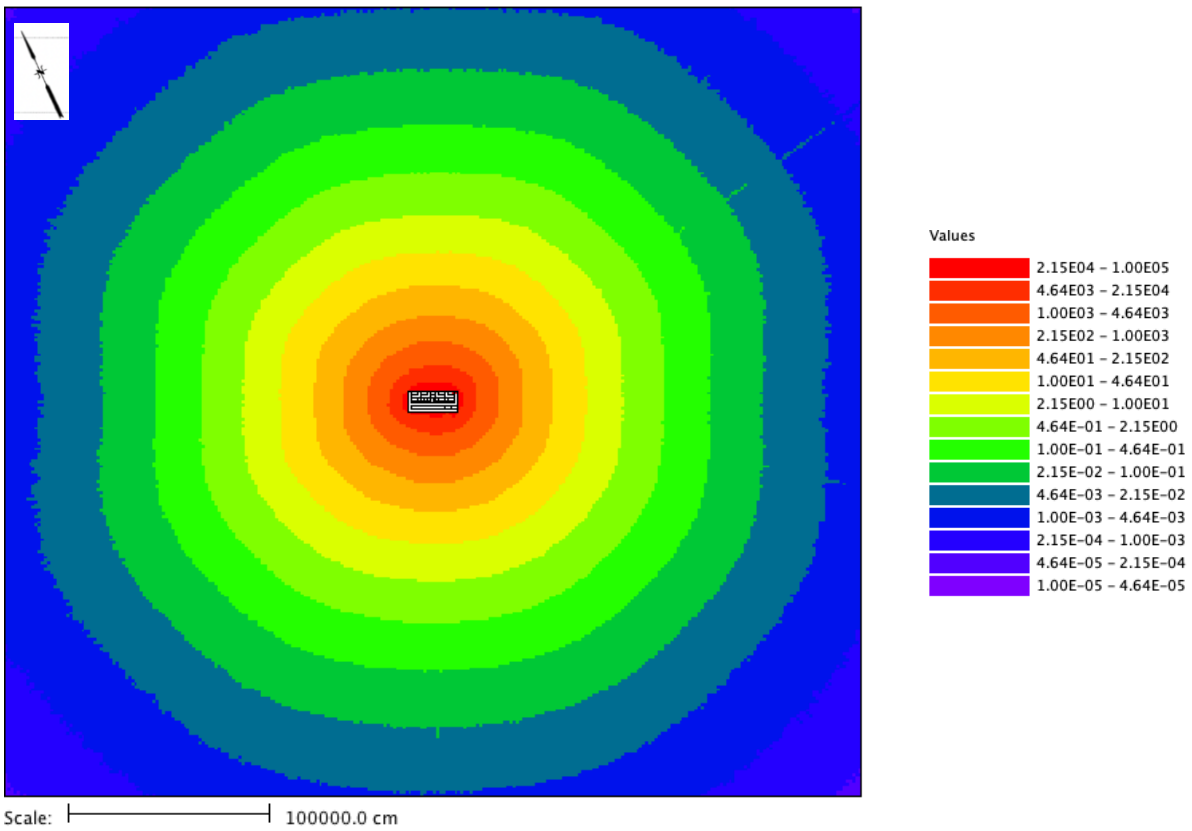

Figure 14. Annual dose (mrem) for area surrounding the Phase 1 storage pad. Total area shown is 4.244 × 4.107 km^2.

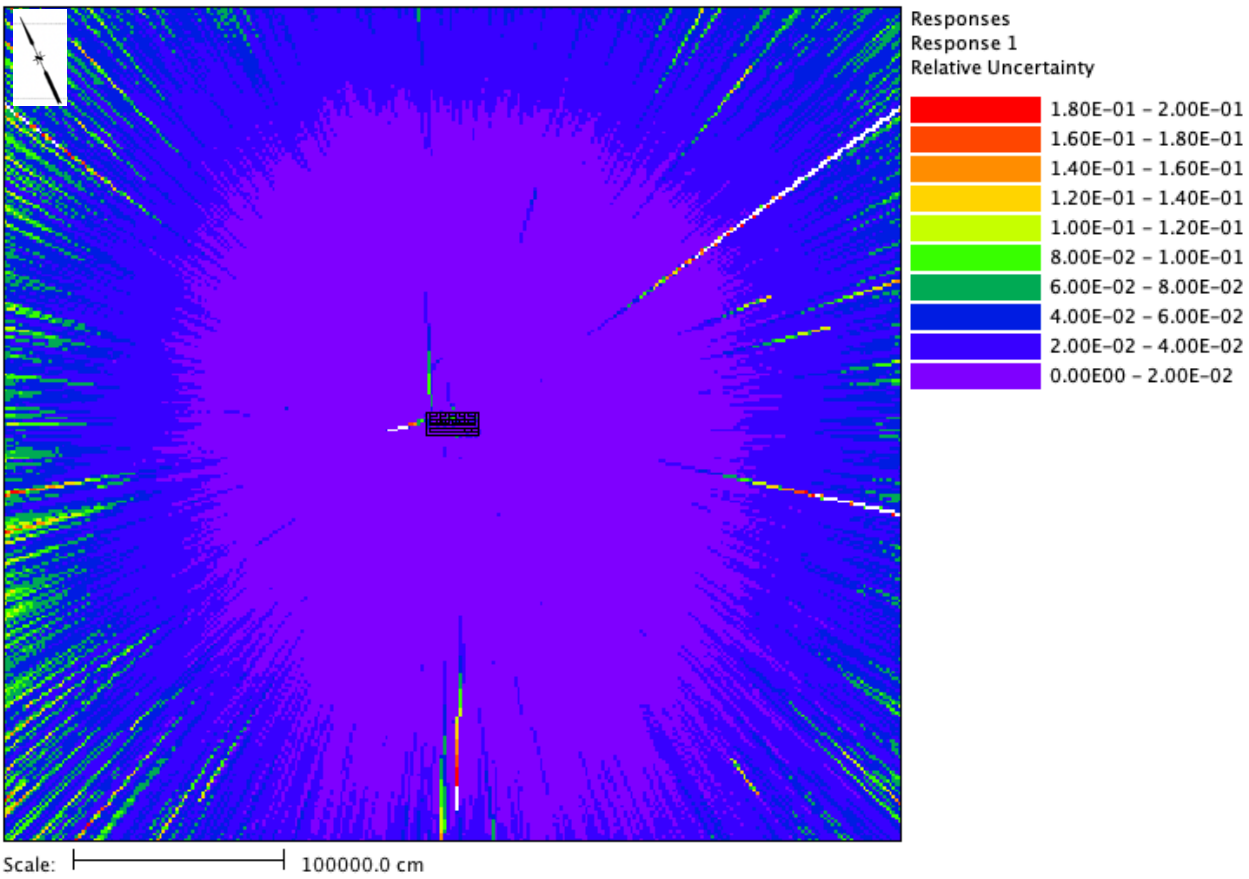

Figure 15. Relative statistical error associated with annual dose values shown in Figure 14.

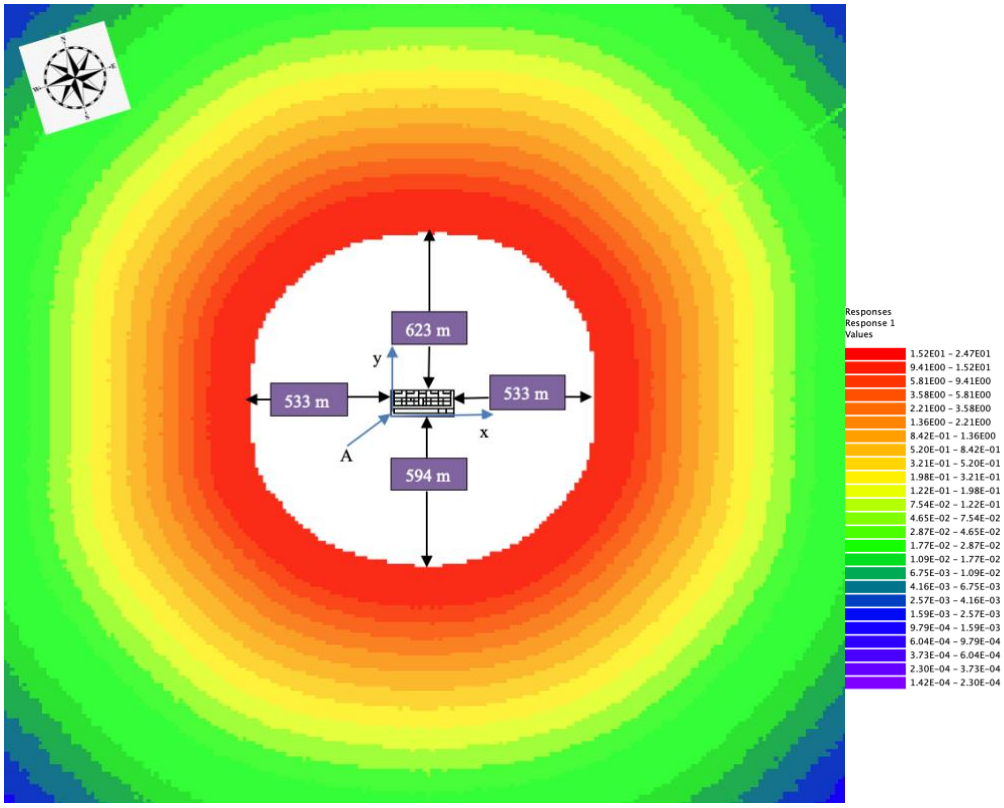

Figure 16. Dose map showing the annual dose (mrem) and the distances from the pad boundary to the 25-mrem/yr contour for the 5,000-MTHM WCS Phase 1 CISF.

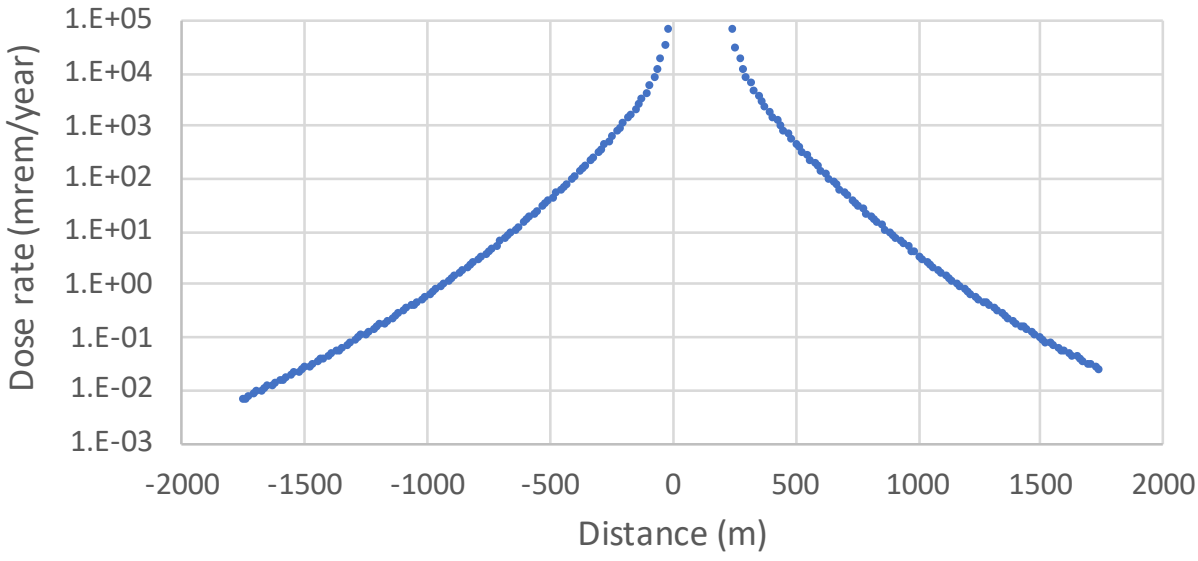

Figure 17. Dose rate along the X axis as a function of distance from the Phase 1 storage pad boundary.

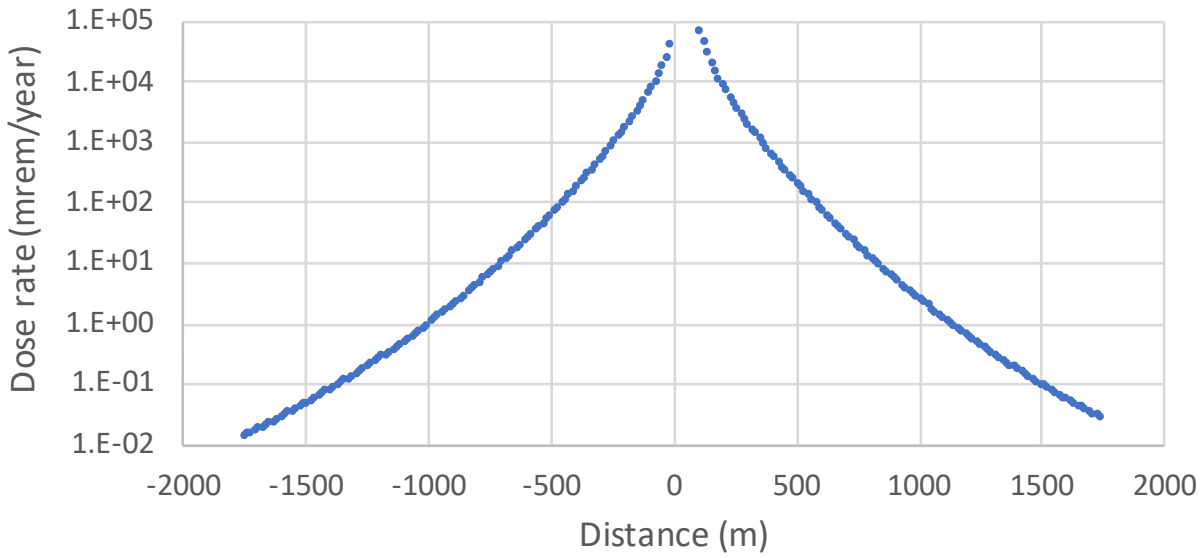

Figure 18. Dose rate along the Y axis as a function of distance from the Phase 1 storage pad boundary.

6. COMPARISON WITH SAR DOSE RATE VALUES

6.1 DOSE RATES AROUND THE WCS CISF

A comparison to dose rate values reported in the SAR (Ref. 2, Table 9-5) for the detector locations D1 through D16 identified in (Ref. 2, Figure 9-1) is presented in Table 5. The radiation dose at the detector locations is produced by the WCS Phase 1 CISF. The locations of these detectors are on the protected area boundary, which is a rectangle enclosing the WCS CISF. This comparison shows that the SAR determined higher annual dose values for detectors D1 through D14 by 12% to 45% and lower annual dose values for detectors D15 and D16 by 18% and 8%, respectively as compared with this ORNL confirmatory calculation.

Table 5. Dose rate comparison for selected detector locations

Detector	Detector location coordinates[a]		Dose rate (mrem/h)		
	X (m)	Y (m)	Safety analysis (Ref. 2, Table 9-5)	This study	Dose rate ratio[b]
D1	-101	122	5.76E-1 ± 1%	4.10E-1 ± 0.6%	1.41 ± 1.7%
D2	-101	244	2.20E-1 ± 2%	1.76E-1 ± 0.5%	1.25 ± 2.6%
D3	-101	366	7.67E-2 ± 4%	5.65E-2 ± 0.5%	1.36 ± 5.5%
D4	-101	488	2.36E-2 ± 2%	1.85E-2 ± 0.5%	1.27 ± 2.6%
D5	-101	619	7.95E-3 ± 5%	5.50E-3 ± 0.6%	1.45 ± 7.3%
D6	122	619	1.04E-2 ± 3%	7.65E-3 ± 0.5%	1.36 ± 4.1%
D7	259	619	9.21E-3 ± 2%	7.25E-3 ± 0.6%	1.27 ± 2.6%
D8	396	619	6.65E-3 ± 3%	5.13E-3 ± 0.6%	1.30 ± 4.0%
D9	619	619	2.22E-3 ± 2%	1.83E-3 ± 0.7%	1.22 ± 2.6%
D10	619	488	5.16E-3 ± 5%	4.19E-3 ± 0.6%	1.23 ± 6.2%
D11	619	366	1.02E-3 ± 4%	8.22E-3 ± 0.6%	1.24 ± 5.0%
D12	619	244	1.47E-2 ± 2%	1.31E-3 ± 0.7%	1.12 ± 2.4%
D13	619	122	1.65E-2 ± 2%	1.45E-2 ± 1.0%	1.14 ± 2.5%
D14	396	-122	1.06E-2 ± 2%	9.20E-2 ± 0.5%	1.15 ± 2.4%
D15	259	-122	2.98E-1 ± 1%	3.64E-1 ± 0.7%	0.82 ± 1.0%
D16	122	-122	4.97E-1 ± 1%	5.41E-1 ± 0.7%	0.92 ± 1.1%

[a]Relative to storage pad corner A identified in Figure 16, the coordinates of which are X=0 m and Y=0 m.

[b]Ratio of SAR dose rate value to dose rate value obtained in this study and associated percent error.

6.2 ANNUAL SITE BOUNDARY DOSE FOR PHASE 1 CISF

The SAR indicates that the minimum distance between site boundary and the CISF is ~ 0.75 miles (1.2 km). An estimated annual site boundary dose for Phase 1 CISF of 7.52E-2 mrem is provided in the SAR (Ref. 2, Section 9.6.1), which includes 7.73E-03 mrem due to postulated leakage of the FO-, FC-, and FF-canisters. Therefore, the estimated annual dose from direct radiation associated with the Phase 1 CISF was 6.747E-02 mrem. An annual site boundary dose of 6.02E-02 ± 2.0E-04 mrem from CISF Phase 1 direct radiation was estimated in this analysis.

7. CONCLUSIONS

This report presents a confirmatory dose rate calculation for the proposed consolidated interim SNF CISF to support an NRC review of the license application submitted by the Interim Storage Partners WCS. The scope of this report is limited to an assessment of the annual dose in air for Phase 1 of the WCS CISF and determination of the controlled area boundary based on the 10 CFR 72.104 annual dose limit to whole body of 25 mrem.

The confirmatory dose rate calculations used the source term and shielding calculation capabilities of the SCALE 6.2.3 computer code system [15]. The calculation method employed in the confirmatory calculations uses a detailed Monte Carlo radiation transport simulation from source to dose rate. This method differs from the two-step method used in the SAR,[2] which requires determination of the photon and neutron energy and angular distributions on the cask external surface and then the use of this surface source in a new radiation transport calculation to determine dose rate as a function of distance from the storage facility. However, for consistency with the SAR, basic input data and assumptions used in the SAR (e.g., cask design parameter and design basis assembly characteristics) were used in this confirmatory calculation. A simulation was made using the complete site geometry (all casks present) but with only one cask containing source. A total of 467 independent calculations were performed to obtain the dose rate maps produced by each storage cask. The size of the model was $4.2 \times 4.1 \times 2.0$ km^3. The local atmospheric conditions were simulated using US standard atmosphere data that provide air temperature, pressure, and density as a function of altitude for a standard atmosphere model. The air column in the geometry model was subdivided into 40 vertical layers, each layer 50 m high, with decreasing air density values from 1.1171 kg/m^3 at the facility level to 0.91382 kg/m^3 at the top of the 2-km thick air layer.

The determined minimum required distances from the WCS Phase 1 CISF to a contour defined by the 25 mrem annual dose limit were approximately 623 m (0.387 miles) in the N-NE direction, 594 m (0.369 miles) in the S-SW direction, and 533 m (0.331 miles) in the E-SE direction and the W-NW direction. The estimated annual dose for the site boundary, 0.75 miles away from the Phase 1 CISF, was approximately 6.02E-02 ± 2.0E-04 mrem, which is significantly smaller than the 25 mrem annual dose limit provided in 10 CFR 72.104. A comparison with the dose rate values reported in the SAR (Ref. 2, Table 9-5) for the detector locations D1 through D16 identified in (Ref. 2, Figure 9-1) is also included in this report. The locations of these detectors were on the protected area boundary, which is a rectangle enclosing the WCS CISF. This comparison shows that the SAR determined higher annual dose values for detectors D1 through D14 by 12% to 45% and lower annual dose values for detectors D15 and D16 by 18% and 8%, respectively as compared with this ORNL confirmatory calculation.

Dose rate sensitivity to air volume, density, and humidity was analyzed because these modeling parameters may affect the dose rate results of skyshine calculations. The complete site geometry and a single VCC containing Connecticut Yankee SNF sources were used in sensitivity calculations. The dose rate values obtained with model sizes of $2.7 \times 2.6 \times 0.96$ km^3 and $4.2 \times 4.1 \times 2.0$ km^3 only differed within their statistical uncertainty, showing that the ample air volume of the CISF model was adequate. Local atmospheric conditions were simulated using US standard atmosphere data, which provide average air temperature, pressure, and density as a function of altitude for a standard atmosphere model. The dose rate calculations simulating local atmospheric conditions indicated that the uniform dry air with a mass density of 1.2 kg/m^3 would not be conservative with respect to dose rate at great distances from the CISF. The lower air density corresponding to local atmospheric conditions produced higher dose rate at locations far away from the analyzed cask relative to the base case of 1.2 kg/m^3. This dose rate increase varied from ~ 45% at 1 km to ~ 70% at 1.7 km from the cask. Air humidity was demonstrated to have negligible effects on dose rate values for simulated local atmospheric conditions.

8. REFERENCES

1. Interim Storage Partners Waste Control Specialists. 2018. *Application for a License for a Consolidated Interim Storage Facility*. ML16133A134, Rev. 2.
2. *WCS Consolidated Interim Storage Facility Safety Analysis Report*, Docket Number 72-1050, Revision 3, Interim Storage Partners, LLC (2020).
3. US Government Publishing Office, 2006. *10 CFR 72 – License Requirements for the Independent Storage of Spent Nuclear Fuel, High-Level Radioactive Waste, and Reactor-Related Greater that Class C Waste*. Washington, DC.
4. NAC International. *Safety Analysis Report for the UMS® Universal Transport Cask*, Rev. 2, CoC 9270 Rev. 4. USNRC Docket Number 71-9270.
5. NAC International. *Final Safety Analysis Report for the UMS Universal Storage System*, Rev. 10, CoC 72-1015 Rev. 5. USNRC Docket Number 72-1015.
6. NAC International. *NAC-STC, NAC Storage Transport Cask Safety Analysis Report*, Rev. 17, CoC 9235 Rev. 13. USNRC Docket Number 71-9235.
7. NAC International. *NAC Multipurpose Cask Final Safety Analysis Report*, Rev. 10, CoC 1025 Rev. 6. USNRC Docket Number 72-1025.
8. NAC International. *MAGNASTOR® Final Safety Analysis Report*, Rev. 6, CoC 1031 Rev. 4. USNRC Docket Number 72-1031.
9. NAC International. *Safety Analysis Report for the MAGNATRAN Transport Cask*, Revs. 12A, 14A, and 15A. USNRC Docket Number 71-9356.
10. TN Americas. *NUHOMS®-MP187 Multi-Purpose Transportation Package Safety Analysis Report*. NUH-05-151 Rev. 17. NRC Docket No. 71-9255.
11. TN Americas. *Rancho Seco Independent Spent Fuel Storage Installation, Final Safety Analysis Report, Volume I, ISFSI System*. NRC Docket No. 72-11, Rev. 4.
12. TN Americas. *NUHOMS® -MP197 Transportation Package Safety Analysis Report*. NRC Docket No. 71-9302. NUH09.101 Rev. 17.
13. TN Americas. *Updated Final Safety Analysis Report for the Standardized Advanced NUHOMS® Horizontal Modular Storage System for Irradiated Nuclear Fuel*. NRC Docket No. 72-1029, ANUH-01.0150. Rev. 6.
14. TN Americas. *Updated Final Safety Analysis Report for the Standardized NUHOMS® Horizontal Modular Storage System for Irradiated Nuclear Fuel*. NRC Docket No. 72-1004. NUH-003. Rev. 14.
15. B. T. Rearden and M. A. Jessee, Eds. 2016. *SCALE Code System*, ORNL/TM-2005/39, Version 6.2.1, Oak Ridge National Laboratory. Available from the Radiation Safety Information Computational Center as CCC-834.
16. W. A. Wieselquist, A. B. Thompson, J. L. Peterson, and S. M. Bowman. April 2016. *ORIGAMI Automator Primer: Automated ORIGEN Source Terms and Spent Fuel Storage Pool Analysis*. ORNL/TM-2015/409, Oak Ridge National Laboratory (2015).
17. G. Radulescu, K. Banerjee, R. A. Lefebvre, L. P. Miller, and J. M. Scaglione. 2017. "Shielding Analysis Capability of UNF-ST&DARDS." *Nucl. Technol*. 199(3): 276–288.

18. R. A. Lefebvre, P. Miller, J. M. Scaglione, K. Banerjee, J. L. Peterson, and G. Radulescu. 2017. "Development of Streamlined Nuclear Safety Analysis Tool for Spent Nuclear Fuel Applications." *Nucl. Technol*. 199(3): 227–244.
19. M. D. DeHart, *Sensitivity and Parametric Evaluations of Significant Aspects of Burnup Credit for PWR Spent Fuel Packages*, ORNL/TM-12973, Oak Ridge National Laboratory (1996).
20. B. L. Broadhead, *Recommendations for Shielding Evaluations for Transportation and Storage*, NUREG/CR-6802, ORNL/TM-2002/31, US Nuclear Regulatory Commission, Oak Ridge National Laboratory (2003).
21. B. L. Broadhead et al., *Investigation of Nuclide Importance to Functional Requirements Related to Transport and Long-Term Storage of LWR Spent Fuel*, ORNL/TM-12742, Oak Ridge National Laboratory (1995).
22. I. C. Gauld and J. C. Ryman, *Nuclide Importance to Criticality Safety, Decay Heating, and Source Terms Related to Transport and Interim Storage of High-Burnup LWR Fuel*, NUREG/CR-6700, ORNL/TM-2000/284, US Nuclear Regulatory Commission, Oak Ridge National Laboratory (2000).
23. J. K. Shultis, "Hybrid Skyshine Calculations for Complex Neutron and Gamma Ray Sources," *Nucl. Sci. and Eng.* **136**, 294–304 (2000).
24. D. E. Peplow. 2011. "Monte Carlo Shielding Analysis Capabilities with MAVRIC." *Nucl. Technol.* 174(2): 289–313.
25. J. C. Wagner, D. E. Peplow, and S. W. Mosher. 2014. "FW-CADIS Method for Global and Regional Variance Reduction of Monte Carlo Radiation Transport Calculations." *Nucl. Sci. Eng.*, 176(1): 37–57.
26. T. M. Evans, A. S. Stafford, R. N. Slaybaugh, and K. T. Clarno. 2010. "Denovo: A New Three-Dimensional Parallel Discrete Ordinates Code In SCALE." *Nucl. Technol.* 171(2): 171–200.
27. American Nuclear Society. 1977. *American National Standard Neutron and Gamma-Ray Flux-to-Dose-Rate Factors*. ANSI/ANS 6.1.1-1977.
28. Waste Control Specialists. 2016. *Supplemental Information to Support a License Application for a Consolidated Interim Storage Facility for Spent Nuclear Fuel in Andrews, Texas*. Rockville, MD.
29. Energy Information Administration. Oct. 2004. *RW-859 Nuclear Fuel Data*. Washington, DC.
30. U.S. Standard Atmosphere 1976 – National Aeronautics and Space Administration, US Government Printing Office, Washington DC (1976).
31. R. J. McConn Jr. et al., Compendium of Material Composition Data for Radiation Transport Modeling, PNNL-15870 Rev. 1, Pacific Northwest National Laboratory (2011).
32. G. Radulescu and K. J. Connolly, "A Parametric Analysis of Factors Affecting Calculations of Estimated Dose Rates from Spent Nuclear Fuel Shipments," Proc. of the WM2016 Conference, Phoenix, Arizona, March 6-10, 2016.
33. https://barani.biz/apps/air-density.